Atmósfera (1989), **2**, p.p. 131-154

Folded resonance and seasonal vacillation in a thermally-forced baroclinic wave model

BARRY SALTZMAN

Dept. of Geology and Geophysics, Yale University, P. O. Box 6666, New Haven, CT 06511

CHUNG-MUH TANG

Universities Space Research Association. The American City Building, Suite 212, Columbia, MD 21044

KIRK A. MAASCH

Dept. of Geology and Geophysics, Yale University, P. O. Box 6666, New Haven, CT 06511

(Manuscript received October 14, 1988; accepted in final form January 23, 1989)

RESUMEN

Un modelo de tres componentes, algo más general que el propuesto recientemente por Lorenz, se estudia con el propósito de ilustrar las posibilidades de la interacción casi-resonante entre ondas largas baroclínicas y el forzamiento térmico de tipo monzón. Se demuestra que el modelo es capaz de exhibir una "resonancia plegada", retrato de equilibrio sugerente de lo que aparece como un requerimiento para explicar la bimodalidad observada de la amplitud de las ondas largas atmosféricas. Uno de los modos está asociado con una onda estable y equilibrada, térmicamente forzada, mientras que el otro está asociado con un ciclo límite estable alrededor de un equilibrio inestable. Este ciclo límite es activado en invierno y conduce a fluctuaciones vacilantes caracterizadas por una larga permanencia en un estado de alta amplitud y fase fija que puede corresponder a uno de los dos modos observados.

ABSTRACT

A three component model, somewhat more general than a recent model of Lorenz, is studied in order to illustrate the possibilities for quasi-resonant interaction of long baroclinic waves and thermal-monsoonal forcing. The model is shown to be capable of exhibiting a "folded resonance" equilibrium portrait suggestive of that which seems to be required to account for the observed bimodality of the atmospheric long-wave amplitude. One of the modes is associated with a stable, equilibrated, thermally forced wave, while the other is associated with a stable limit cycle about an unstable equilibrium. This limit cycle is activated in winter, leading to vacillatory fluctuations characterized by a long residence in a state of high amplitude and fixed phase that may correspond to one of the two modes observed.

1. Introduction

Statistical analyses of observations show that the largest scales of planetary atmospheric flow possess a bimodal wave amplitude probability structure (Sutera, 1986; Hansen, 1986), that the two modes are baroclinic (Hansen and Sutera, 1986; Hansen, 1988), and that in winter there tends to be quasi-periodic major outbreaks of cold continental air apparently associated with the high amplitude mode having a most probable period near 20 days (e.g., McGuirk and Reiter, 1976; Schilling, 1987).

Our aim here is to explore the degree to which these features can be accounted for, at least qualitatively, within the framework of simple 3-variable low-order dynamical model driven only by

seasonally varying heating (i.e., by thermal-monsoonal, as opposed to orographic, effects). As a basis for this model in the next section we first outline the derivation of a more general 8-variable dynamical system including as special cases not only our present model, but nearly all low-order models studied to date that exclude wave-wave interactions.

2. A generalized low-order, quasi-geostrophic model

The fundamental quasi-geostrophic equations can be written in the form (e.g., McWilliams and Gent, 1980)

$$\frac{\partial u}{\partial t} + u\frac{\partial u}{\partial x} + v\frac{\partial u}{\partial y} - f_o v_\chi - F_x = 0 \tag{2.1}$$

$$\frac{\partial v}{\partial t} + u\frac{\partial v}{\partial x} + v\frac{\partial v}{\partial y} + f_o u_\chi + \frac{\beta}{f_o}\phi - F_y = 0 \tag{2.2}$$

$$\frac{\partial \phi}{\partial p} + \frac{RT}{p} = 0 \tag{2.3}$$

$$\frac{\partial T}{\partial t} + u\frac{\partial T}{\partial x} + v\frac{\partial T}{\partial y} - S_p\omega - \frac{q}{c_p} = 0 \tag{2.4}$$

$$\frac{\partial \omega}{\partial p} + \frac{\partial u_\chi}{\partial x} + \frac{\partial v_\chi}{\partial y} = 0 \quad , \quad \frac{\partial u}{\partial x} + \frac{\partial v}{\partial y} = 0 \tag{2.5a,b}$$

with boundary conditions,

$$\omega = 0 \quad \text{at} \quad p = 0 \tag{2.6}$$

$$\omega_s = -\rho_s g(V_s \cdot \nabla h),$$

$$(\tau_x \ , \ \tau_y)_s = \rho_s C^*(u_s \ , \ v_s) \quad \text{at} \quad p = p_s \tag{2.7a,b}$$

where $(x,\ y)$ are the Cartesian zonal and meridional distance coordinates, p is pressure, $(v,\ v)$ and $(u_\chi,\ v_\chi)$ are the zonal and meridional non-divergent (quasi-geostrophic) and irrotational components of the wind, respectively, T is temperature, ϕ is geopotential, $\omega = dp/dt$, q is the rate of heating per unit mass, $(F_x,\ F_y) = -\nu(u,\ v) = -g\frac{\partial}{\partial p}(\tau_x,\ \tau_y)$, ν is a Rayleigh friction coefficient, $(\tau_x,\ \tau_y)$ are the viscous stresses, C^* is the surface friction constant, f_o is a representative middle latitude Coriolis parameter, $\beta = \partial f/\partial y$, g is gravity, R is the gas constant, c_p is the specific heat at constant pressure, $S_p = -T\theta^{-1}\partial\theta/\partial p$ (θ = potential temperature), h is the topographic height, and the subscript s denotes surface values.

Let us now do the following:

1. Define a vertical average $\widehat{(\ )}$ applicable in the mid-troposphere ($\sim$ 500 mb), a zonal average $\overline{(\ )} = (\ \ )$ - $(\ \ )'$, and a global average $(\ \tilde{}\ )$,

2. Apply the system to a β-channel of width D, and periodic zonal wavelength L representing a continent-ocean scale ($k = 2\pi/L$, $l = \pi/D$), with no topographic variations (h=0), ground surface temperature T_s, basic radiative heating $R(y)$, and a compatible "shape assumption"-wave structure of the forms,

$$T_s(x,y) = T_{so} - B_{so}y + C_{so} \sin 2ly + C_{s2} \cos kx \sin ly \tag{2.8}$$

$$R(y) = R(0) - R_o y \tag{2.9}$$

$$\hat{v}(x,y) = (V_1 \sin kx + V_2 \cos kx)\sin ly \tag{2.10}$$

$$\hat{u}(x,y) = (U_o - U_1 \cos 2ly) + \frac{l}{k}(V_1 \cos kx - V_2 \sin kx) \cos ly \tag{2.11}$$

$$\hat{T}(x,y) = (T_o - B_o y + C_o \sin 2ly) + (C_1 \sin kx + C_2 \cos kx)\sin ly \tag{2.12}$$

$$(-\frac{\partial \overline{\hat{T}}}{\partial y}) = B_o - B \cos 2ly \quad , \quad B = 2lC_o \tag{2.14a,b}$$

$$\omega(x,y,p) = \Omega(x,y)\sin \frac{\pi}{p_s}p + \omega_s(x,y)(\frac{p}{p_s})^2 \tag{2.14}$$

We shall assume that L and D are of magnitudes that are identifiable with the major long-wave systems over a sector including North America and the adjacent portions of the Atlantic and Pacific oceans. In addition, we make the following further assumptions,

3. that the poleward eddy momentum transport, due to wave structure and wave-wave interactions not explicitly represented in this model, is of the form

$$\overline{u'v'} = M(0) - M_o y + M_1 \sin 2ly, \tag{2.15}$$

4. that we can neglect the effects on atmospheric temperature of vertical motions driven by viscosity, and

5. that the heating due to short and long wave radiation, vertical convection, latent heat release, and small and cyclone-scale diffusion can be parameterized in the simplified form,

$$\frac{\hat{q}}{c_p} = R(y) + K\frac{\partial^2 \overline{\hat{T}}}{\partial y^2} + \alpha_1 T_s - \alpha_2 \hat{T} + \alpha_3 \frac{\partial \hat{T}}{\partial x} + \alpha_4 \tag{2.16}$$

where $R(y)$ is the absorbed shortwave radiation, K is a diffusivity for the effects of shorter cyclone-scale baroclinic waves, $(\alpha_1 T_s - \alpha_2 \hat{T})$ measures the effects of all subsynoptic modes of convection and longwave radiation under zonal-mean cloud conditions, the fifth term is meant to represent the effects of latent heat release and cloud-induced long wave radiative warming along storm tracks associated with the planetary-wave structure (e.g., Ramanathan, 1987), and α_4 is a constant.

With these approximations, we obtain the following 8-variable dynamical system:

$$\frac{dV_1}{dt} = k(U_o + \lambda_o U_1)V_2 - \frac{k}{\mu^2}\beta V_2 + \lambda_1(B_o + \lambda_o B)C_1 - \nu V_1 \tag{2.17}$$

$$\frac{dV_2}{dt} = -k(U_o + \lambda_o U_1)V_1 + \frac{k}{\mu^2}\beta V_1 + \lambda_1(B_o + \lambda_o B)C_2 - \nu V_2 \tag{2.18}$$

$$\frac{dC_1}{dt} = k[U_o + \frac{1}{3}(1 - \lambda_2)U_1]C_2 - \lambda_3 C_2 + [\lambda_4 B_o + \frac{1}{3}(\lambda_2 + \lambda_4)B]V_1 - \kappa_1^* C_1 \tag{2.19}$$

$$\frac{dC_2}{dt} = -k[U_o + \frac{1}{3}(1 - \lambda_2)U_1]C_1 + \lambda_3 C_1 + [\lambda_4 B_o + \frac{1}{3}(\lambda_2 + \lambda_4)B]V_2 - \kappa_1^* C_2 + \mathcal{G} \tag{2.20}$$

$$\frac{dU_1}{dt} = M - \nu^*(U_1 - \frac{R}{f_o}B) \tag{2.21}$$

$$\frac{dU_o}{dt} = \mathcal{M}_o - \nu^*(U_o - \frac{R}{f_o}B_o) \tag{2.22}$$

$$\frac{dB}{dt} = -\lambda_5(V_1 C_1 + V_2 C_2) - \kappa_2^* B + \mathcal{F} \tag{2.23}$$

$$\frac{dB_o}{dt} = R_o - \alpha_2 B_o + \mathcal{F}_o \tag{2.24}$$

where, if we define

$$\mu^2 = k^2 + l^2$$

$$\gamma = \frac{2Rp_s S_p}{\pi^2 f_o^2}$$

$$\xi = (2 + \frac{\pi^2}{4})p_s^{-2}$$

the source functions are given by

$$\mathcal{G} = \frac{\alpha_1 C_{s2}}{(1 + \gamma\mu^2)}$$

$$M = 2l\mathcal{M}_1$$

$$\mathcal{F} = \frac{\alpha_1 C_{so}}{(1 + 2\gamma l^2)}$$

$$\mathcal{F}_o = -\alpha_1 B_{so}$$

and the coefficients are

$$\kappa_1^* = \alpha_2/(1+\gamma\mu^2)$$

$$\kappa_2^* = (\alpha_2 + 4l^2K)/(1+2l\gamma)$$

$$\nu^* = gC^*/R\tilde{T}_s$$

$$\lambda_o = (k^2 - 3l^2)/3\mu^2$$

$$\lambda_1 = (R^2k^2)/3f_o^2$$

$$\lambda_2 = 4l^2\gamma/(1+\gamma\mu^2)$$

$$\lambda_3 = k(\gamma\beta + \alpha_3)/(1+\gamma\mu^2)$$

$$\lambda_4 = (1-\gamma\mu^2)/(1+\gamma\mu^2)$$

$$\lambda_5 = l^2/(1+2\gamma l^2)$$

Each of the above eight equations can be made more realistic by adding terms representing stochastic forcing (e.g., Egger, 1981). Although the above system excludes all possibilities for ageostrophic behavior (e.g., frontal formation) and for explicit wave-wave interactions, it does allow for strongly nonlinear interaction between a single finite-amplitude planetary broclinic wave and a zonal mean thermal and wind state described by two spatial modes. The inclusion of heating and viscosity permits the system to exhibit multiple steady-states that can be stable or unstable and hence be capable, in principle, of giving first order representation of all the observed phenomena described in the Introduction. As noted in the Introduction, the model can be specialized to yield many of the previously considered low order models: Note that these quasi-geostrophic equations can easily be rewritten in terms of a streamfunction, e.g., $u = -\partial\psi/\partial y$, $v = \partial\psi/\partial x$, where $\psi = \overline{\psi} + k^{-1}(V_2 \sin kx - V_1 \cos kx) \sin ly$. For example, if we set $U_o = B_o = 0$ and postulate that $(V_1, V_2, U_1) \sim (C_1, C_2, B_1)$, we obtain the simple 3-variable baroclinic model of the type recently discussed by Lorenz (1984).

In the present study we shall enlarge upon this latter Lorenz model by allowing (i) for a richer variability of the zonal mean state by allowing $U_o \sim B_o \neq 0$ in the spirit of the Rambaldi - Mo (1984) barotropic study, (ii) for the effect of β on the thermal field, (iii) for an additional free internal heat source if $\alpha_3 \neq 0$, and (iv) for implicit dynamical effects that tend to drive the system toward an equivalent barotropic state.

3. A thermally-driven three-variable, baroclinic model

We reduce the system (2.17) - (2.24) by assuming that the wind field is related diagnostically to the thermal field by the relationships:

$$U_o = \frac{R}{f_o} B_o \tag{3.1}$$

$$U_1 = m \frac{R}{f_o} B \tag{3.2}$$

$$V_1 = \Phi C_1 - \Psi C_2 \tag{3.3}$$

$$V_2 = \Phi C_2 + \Psi C_1 \tag{3.4}$$

where m, Φ, and Ψ are positive constants.

Equations (3.1) and (3.2), expressing the strong relation between the strength of the mean zonal winds and the mean baroclinicity, derive from the steady state versions of (2.21) and (2.22). Assuming the "negative viscosity" effect (M > 0) implied by the Saltzman-Vernekar (1968) parameterization of $\overline{u'v'}$, it follows that we can reasonably set $m \approx 1.2$.

Equations (3.3) and (3.4) express the possibility for resolving the wave motions in terms of a baroclinic part measured by Φ (geostrophic streamlines 90 degrees out of phase with vertical mean isotherms leading to a tilting of the wave motions with height), and an "equivalent barotropic" part measured by Ψ (streamlines in phase with vertical mean isotherms at all levels and no tilting with height). In the Lorenz (1984) model only the baroclinic component is considered ($\Psi = 0$).

In essence, by writing (3.1) to (3.4) we are assuming that as a first approximation we can consider the wind field to be geostrophically equilibrated to the thermal field by processes not being considered explicitly. Although plausible, the question of the validity of this assumption requires much deeper consideration than we shall provide here, where we shall simply adopt (3.1) - (3.4) as our working postulates forming the foundations of our model as they are of the Lorenz (1984) model. At the least, these relations are qualitatively consistent with the assumption that the thermal damping time is larger than the viscous damping time for planetary waves (e.g., Hendon, 1986; Neelin *et al.*, 1987).

Moreover, assuming that $(\lambda_2/3)B$ is small compared to the basic baroclinicity B_o, it can be demonstrated from (2.17) and (2.18) that for long term mean conditions the eddy kinetic energy is conserved, i.e., $\overline{\overline{d(V_1^2 + V_2^2)}}/dt = 0$, if

$$\Phi = \frac{(Rk)^2 \overline{\overline{B_o}}}{3 f_o^2 \nu (1 + \epsilon^2)} \tag{3.5}$$

where $\overline{\overline{(\quad)}}$ denotes a long time average, and $\epsilon = \Psi/\Phi$.

Using (3.1) - (3.4) we obtain the reduced system

$$\frac{dC_1}{dt} = \mu_1(B_o)C_2 + \mu_2 BC_2 + \mu_3(B_o)C_1 + \mu_4 BC_1 \tag{3.6}$$

$$\frac{dC_2}{dt} = -\mu_1(B_o)C_1 - \mu_2 BC_1 + \mu_3(B_o)C_2 + \mu_4 BC_2 + \mathcal{G} \tag{3.7}$$

$$\frac{dB}{dt} = -\Phi\lambda_5(C_1^2 + C_2^2) - \kappa_2^* B + \mathcal{F} \tag{3.8}$$

$$\frac{dB_o}{dt} = R_o - \alpha_2 B_o - \mathcal{F}_o \tag{3.9}$$

where

$$\mu_1 = (\frac{kR}{f_o} - \Psi\lambda_4)B_o - \lambda_3$$

$$\mu_2 = \frac{1}{3}[k(1-\lambda_2)m\frac{R}{f_o} - \Psi(\lambda_2 + \lambda_4)]$$

$$\mu_3 = (\Phi\lambda_4)B_o - \kappa_1^*$$

$$\mu_4 = \frac{1}{3}\Phi(\lambda_2 + \lambda_4)$$

The last equation states that the basic linear temperature gradient between the equator and pole, B_o, is forced only by radiation and surface heating, independent of any coupling to the other variables, C_1, C_2 and B. Hence (3.9) can be solved separately to yield an expression for the annual variation of B_o in the form,

$$B_o = B_{oo} + B_{o1} \cos \frac{2\pi}{1yr}t \tag{3.10}$$

where $t = 0$ corresponds to the maximum temperature gradient in mid-winter. Thus, we remain with a 3-variable dynamical system governing C_1, C_2, and B, with B_o to be taken either as a seasonally-varying parameter given by (3.10), or as a fixed constant if we choose to neglect the seasonal variation (as might be appropriate for conditions within a fixed season).

We note that at the same time the north-south baroclinicity varies seasonally in accordance with (3.10) it is to be expected that the east-west (i.e., continent-ocean) surface temperature profile measured by C_{s2} also varies seasonally in phase with B_o. Consequently we can set

$$\mathcal{G} = \mathcal{G}_o + \mathcal{G}_1 \cos \frac{2\pi}{1yr}t \tag{3.11}$$

where, again, $t = 0$ corresponds to mid-winter when the ocean is warm relative to the continent.

Nondimensional forms - if we define

$$a = \frac{\kappa_2^*}{\kappa_1^*}$$

$$b = \frac{m(1-\lambda_2)}{3} b^*$$

$$b^* = \frac{kR}{\Phi f_o \lambda_4}$$

$$c = \frac{\Phi \lambda_4 B_o}{\kappa_1^*}$$

$$d = \frac{\lambda_3}{\kappa_1^*}$$

$$e = \frac{\lambda_2 + \lambda_4}{3\lambda_4}$$

$$F = \frac{\Phi \lambda_4}{\kappa_1^* \kappa_2^*} \mathcal{F}$$

$$G = \frac{\Phi(\lambda_4 \lambda_5)^{1/2}}{\kappa_1^{*2}} \mathcal{G}$$

and

$$X = (\frac{\Phi \lambda_4}{\kappa_1^*}) B$$

$$Y = [\frac{\Phi(\lambda_4 \lambda_5)^{1/2}}{\kappa_1^*}] C_2$$

$$Z = [\frac{\Phi(\lambda_4 \lambda_5)^{1/2}}{\kappa_1^*}] C_1$$

$$t^* = \kappa_1^* t$$

equations (3.8), (3.6) and (3.7), respectively, can be written in the nondimensional form,

$$\dot{X} = -Y^2 - Z^2 - aX + aF \tag{3.12}$$

$$\dot{Y} = eXY - K_1 XZ + K_2 Y - K_3 Z + G \tag{3.13}$$

$$\dot{Z} = eXZ + K_1XY + K_2Z + K_3Y \tag{3.14}$$

where $(\dot{\ }) = d(\ )/dt^*$ and the coefficients are given by

$$K_1 = (b - e\epsilon)$$

$$K_2 = [c(B_o) - 1]$$

$$K_3 = [(b^* - e)c(B_o) - d]$$

The model treated by Lorenz (1984) is obtained by setting $e = 1$ and $c = d = \epsilon = 0$ (i.e., $K_1 = b, K_2 = -1$, and $K_3 = 0$). As discussed by Lorenz (1984, 1987) this simplified model already admits a rich and interesting set of solutions, with meaningful implications for the theory of atmospheric motions. We shall proceed to discuss some further consequences of the somewhat more general system (3.12) - (3.14).

4. Steady-states and stability

If we set $\dot{X} = \dot{Y} = \dot{Z} = 0$, and let the corresponding steady-states be denoted by $\hat{X}, \hat{Y}$ and $\hat{Z}$, we have

$$-\hat{Y}^2 - \hat{Z}^2 - a\hat{X} + aF = 0 \tag{4.1}$$

$$[e\hat{X} + K_2(c)]\hat{Y} - [K_1\hat{X} + K_3(c)]\hat{Z} = -G \tag{4.2}$$

$$[e\hat{X} + K_2(c)]\hat{Z} + [K_1\hat{X} + K_3(c)]\hat{Y} = 0 \tag{4.3}$$

which can be solved to give

$$\hat{Y} = \frac{-[e\hat{X} + K_2(c)]G}{P^2} \tag{4.4}$$

$$\hat{Z} = \frac{[K_1\hat{X} + K_3(c)]G}{P^2} \tag{4.5}$$

where $P^2 = \{[e\hat{X} + K_2(c)]^2 + [K_1\hat{X} + K_3(c)]^2\}$ and $\hat{X}$ satisfies the relation

$$a(F - \hat{X})P^2 = G^2 \tag{4.6}$$

Equations (4.4), (4.5) and (4.6) imply that the nondimensional steady-state thermal wave amplitude is

$$\hat{A}^* \equiv (\hat{Y}^2 + \hat{Z}^2)^{1/2} = \frac{G}{P} = [a(F - \hat{X})]^{1/2} \tag{4.7}$$

and the phase angle between the thermal wave and the forcing represented by G is

$$\hat{\theta} = \arctan(\hat{Z}/\hat{Y}). \tag{4.8}$$

In dimensional units the amplitude is given by

$$\hat{A} = \frac{\Phi(\lambda_4\lambda_5)^{1/2}}{\kappa_1^*}(\hat{Y}^2 + \hat{Z}^2)^{1/2}.$$

From (4.7) we see that the condition for quasi-resonance is $P = P_{minimum}$, which in the linear case ($\hat{X} = F$) implies that c (resonance) $= \{(b^* - \epsilon)[d - (b - e\epsilon)F] - eF + 1\}/\{1 + (b^* - \epsilon)^2\}$. Note that if there is no monsoonal forcing ($G = 0$) we have $\hat{A}^* = 0$ (or $\hat{Y} = \hat{Z} = 0$) and $\hat{X} = F$ (the Hadley circulation). With monsoonal forcing ($G \neq 0$), however, a variety of equilibria are possible. To illustrate the possibilities let us adopt the "reference values" of the basic parameters given in Table 1.

Table 1 : Reference Values of Parameters

Basic Constants	Value
g	9.8 m s^{-2}
R	287 m^2 s^{-2} K^{-1}
c_p	10^3 m^2 s^{-2} K^{-1}
a	6.37×10^6 m

Model Parameters	Value
f_0	10^{-4} s^{-1}
β	1.6×10^{-11} m^{-1} s^{-1}
ρ_s	1.2 kg m^{-3}
p_2	500 mb = $.5 \times 10^5$ kg m^{-1} s^{-2}
p_s	1000 mb = 10^5 kg m^{-1} s^{-2}
S_p	5×10^{-4} K m s^2 kg^{-1}
γ	28×10^{10} m^2
T_{s0}	295 K
$\bar{T}_s$	288 K
ξ	4.5×10^{-10} m^2 s^4 K^{-2}
L	9500 km
D	7500 km
ν	$(4d)^{-1}$
κ_1^*	$(6.4d)^{-1}$
κ_2^*	$(3.2d)^{-1}$
α_3	0 m s^{-1}
m	1.2
ϵ	1.2
$\bar{B}_0$	4×10^{-6} K m^{-1}
$\mathcal{F}$	1.34×10^{-11} K m^{-1} s^{-1}
$\mathcal{G}$	0.85 K d^{-1}

Corresponding to these reference values we have the nondimensional values: $a = 2.000$, $b^* = 3.927$, $b = 1.307$, $c(\bar{\bar{B}}_0) = 1.074$, $d = 1.405$, $e = 0.412$, $K_1 = 0.812$, $K_2(\bar{\bar{B}}_o) = 0.074$, $K_3(\bar{\bar{B}}_0) = 1.524$, $F = 1.000$, and $G = 0.700$. From (3.5) we have $\Phi(\bar{\bar{B}}_o) = 0.684$ m s^{-1} K^{-1}. Note that for the reference values, the basic baroclinicity B_0, the east-west thermal forcing $\mathcal{G}$, and the thermal wave amplitude A, are related to the nondimensional numbers c, G, and $A^*(= \sqrt{Y^2 + Z^2})$, respectively, by the formulas,

$$B_o = 3.72 \quad c \qquad (10^{-6} K \quad \mathrm{m}^{-1})$$

$$\mathcal{G} = 1.22 \quad G \quad (K \mathrm{day}^{-1})$$

$$A = 7.83 \quad A^* \qquad (K)$$

Using the method described in Appendix A1 we can obtain the fixed point (or steady-state) values $\hat{X}$, $\hat{Y}$, and $\hat{Z}$. In Fig. 1 we show the implied steady-state nondimensional values of the thermal wave amplitude, $\hat{A}^*$, plotted as a function of the wave forcing, G, for three different values of $c(B_o)$ ranging between the summer and winter values, 0.4 and 1.2 corresponding to $B_o = 1.5$ and 4.5 x 10^{-6} K m^{-1} respectively. As noted by Lorenz (1984), only one steady state "Hadley circulation" can exist

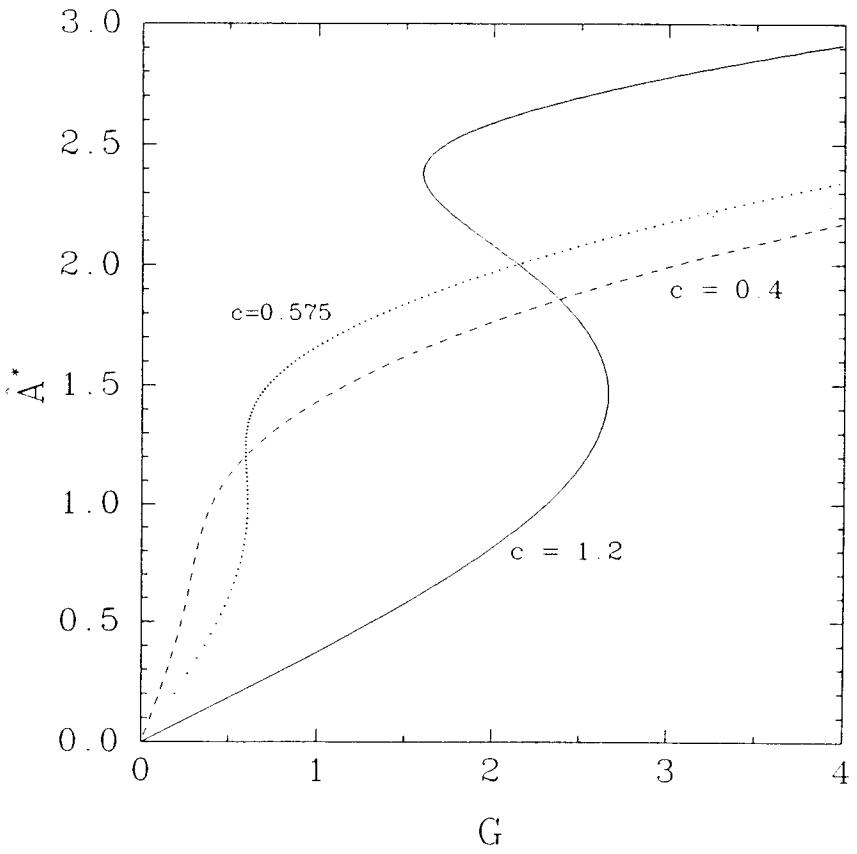

Fig. 1. Steady-state values of the thermal wave amplitude $\hat{A}^*$ as a function of the wave forcing G, for $c = 0.4$, 0.62 and 1.2.

when $G = 0$ (no monsoonal forcing). However, for non-zero values of G multiple steady zonal mean states are possible depending on the value of $c(B_o)$. For example, at our reference value, $G = 0.7$, we find three steady states for $c = 0.62$ (curve not shown in Fig. 1). We note also that this equilibrium portrait bears much similarity to the one described recently by Yoden (1987) in his discussion of stratospheric vacillations, particularly as regards the bifurcation properties to be described below.

In Fig. 2 (solid curve) we show the implied steady-state values of the eddy amplitude, $\hat{A}^*$, as a function of the magnitude of the basic meridional temperature contrast c for the reference atmospheric parameters given in Table 1. The dashed curve represents the steady-states for the case in which Y and Z are assumed to be small enough to justify neglecting $(\hat{Y}^2 + \hat{Z}^2)$ in (4.1), so that $\hat{X} = F$. In this linear case the system admits a classical quasi-resonant steady state centered near $c = 0.27$. The existence of quasi-resonant stationary long waves forced by heating has been discussed by Smagorinsky (1953), Döös (1962), and Saltzman (1965) for a basic zonal atmospheric flow varying continuously in the vertical, and by Derome and Wiin-Nielsen (1971) for a two-layer channel model. However, when non-linearity is retained, with $\hat{X}$ satisfying (4.1), the resulting steady-state (solid) curve is "folded" toward super-resonant values of c admitting three steady states for values of c in a narrow range near 0.62. Such a non-linear resonance has been discussed in a barotropic context by

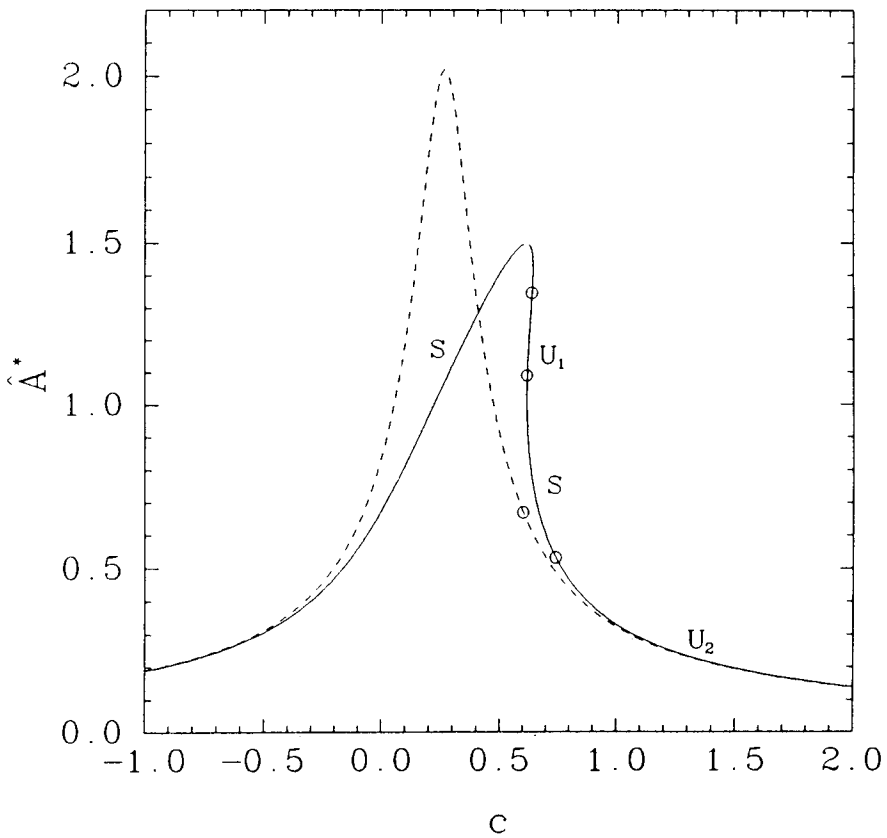

Fig. 2. Steady-state wave amplitude $\hat{A}^*$ as a function of the basic externally-imposed baroclinicity c, for linear (dashed curve) and nonlinear (full curve) cases. On the nonlinear "folded resonance" curve, S denotes a stable equilibrium, U_1 denotes an exponential instability, and U_2 denotes an oscillatory instability.

Trevisan and Buzzi (1980), Malguzzi and Speranza (1981), Rambaldi and Mo (1984), and Speranza (1986) for example. In Fig. 3a, b we show that this folding can be made more striking, for example by increasing the value of the wave forcing, G, or by decreasing ϵ (the ratio of the non-advective to the advective part of the eddy wind field), both of which tend to make the system more nonlinear.

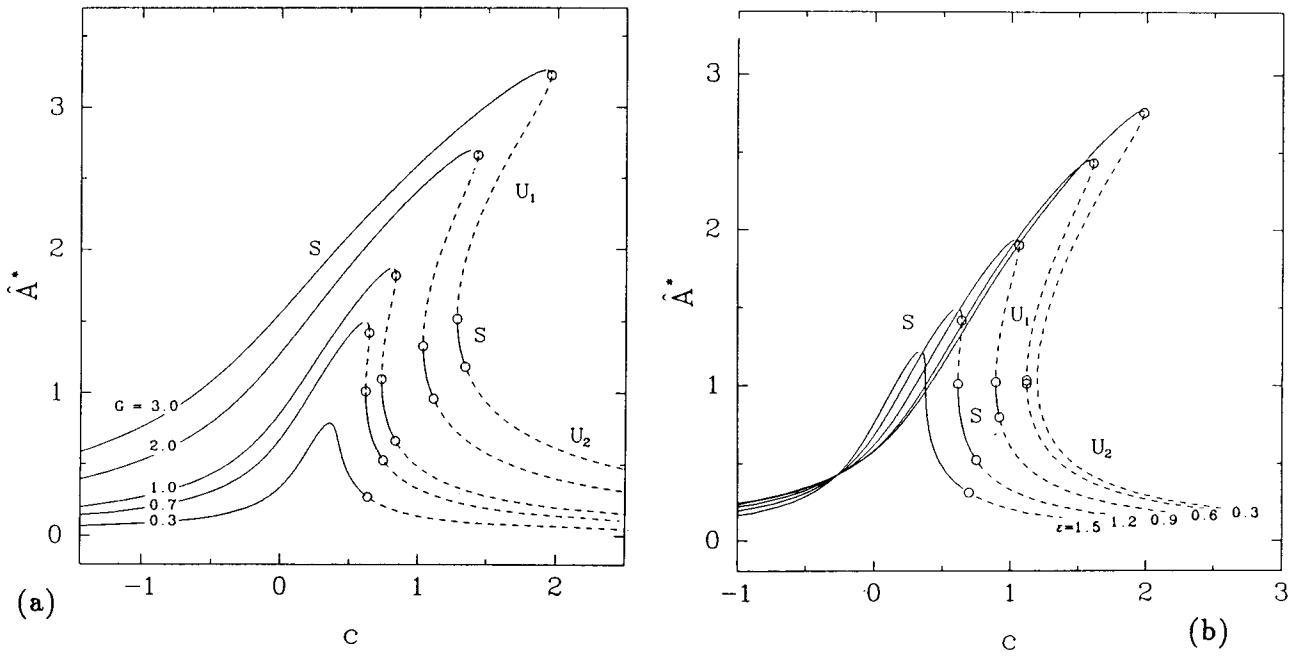

Fig. 3. Steady-state values of the nondimensional wave amplitude $\hat{A}^*$, as a function of the nondimensional basic baroclinicity c, (a) for G = 0.3, 0.7 (the reference value), 1.0, 2.0 and 3.0, and (b) for ϵ = 1.5, 1.2 (the reference value), 0.9, 0.6, and 0.3.

The phase angles given by (4.8), for the reference steady state solutions shown in Fig. 2, are shown in Fig. 4. We note the marked change in phase near the quasi-resonance, with the high - c (winter-like) unstable equilibria leading the wave forcing by about 100 degrees. Thus, according to this model we should expect that in winter the presence of a very low-amplitude wave in which the thermal trough is near the east coast of the continent should be a rare event, owing to the instability of this configuration.

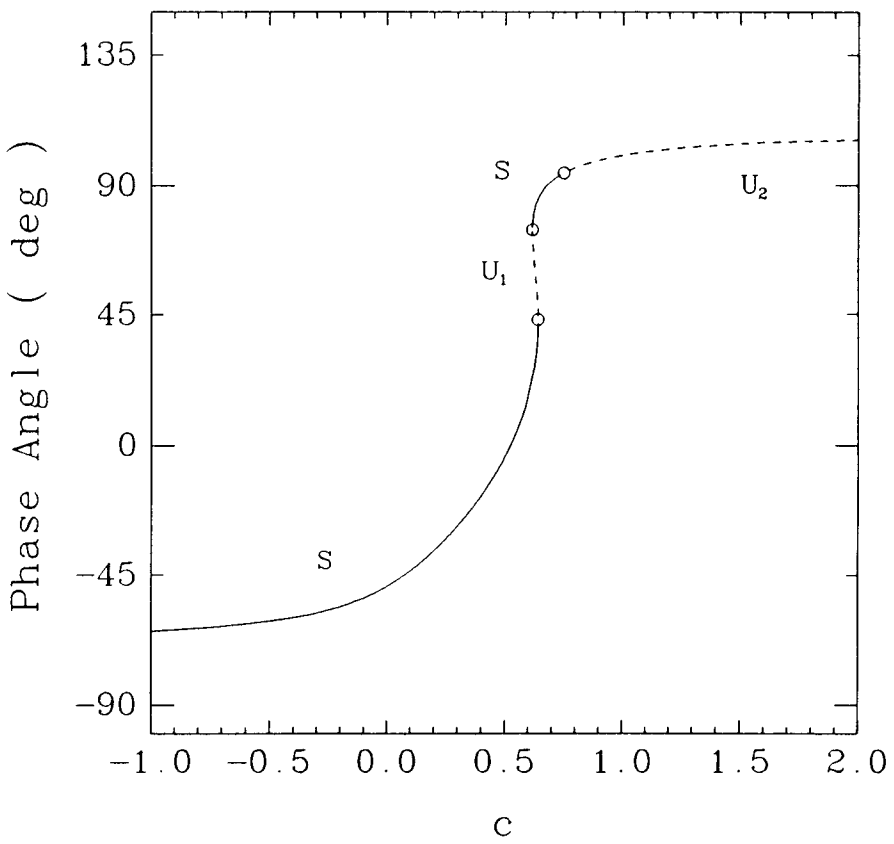

Fig. 4. Steady-state phase angles $\hat{\theta}$, as a function of c, corresponding to the amplitudes shown in Fig. 2.

Stability

The behavior of the system near the above steady-states depends on the eigenvalues of the stability matrix of the system evaluated at these steady states. We obtain these eigenvalues by the method described in Appendix A2. If all eigenvalues have negative real parts the steady-state is stable and will tend to be the attractor for a probability maximum, while if one or more of the eigenvalues have a positive real part the steady-state is unstable and will tend to coincide with a probability minimum. In Fig. 2 we represent our results of such an eigenvalue analysis by denoting spirally-stable portions of the steady-state curve by "S", and unstable portions by "U". In all the stable regions two of the eigenvalues have imaginary parts and are therefore the "spiral" type. The unstable equilibria can be further subdivided into those at which the eigenvalue has no imaginary part (purely exponential amplification) denoted by U_1, and those at which there is an imaginary part (indicative of the nearby Hopf-type bifurcation) denoted by U_2 at which we can expect a stable limit cycle (or vacillatory behavior).

We note again from Fig. 2 that for our reference parameters there exists only a small band of values of c (near 0.62) for which two *stable* equilibria separated by an unstable equilibrium are present.

When the fold is greater, as in the cases shown in Fig. 3a,b, we find that for a given value of c the upper stable equilibrium is usually complemented not by a lower stable equilibrium point but by a spirally-unstable equilibrium point (U_2) that can give rise to a stable limit cycle attractor. In both cases the possibility exists that some form of bimodal wave-amplitude probability distribution can be generated corresponding to a unimodal probability distribution for c, as suggested by the observations. However, as noted by Benzi *et al.* (1987), difficulties arise in accomplishing these transitions in a realistic manner without the presence of additional wave-wave interactions that are not included in our present model.

5. Time dependent behavior: summer monsoon and winter vacillation

From the equilibrium portrait, Fig. 2, we see that for the parameter values adopted, when $c < 0.61$ the system has only a single stable equilibrium and hence cannot exhibit any sustained time dependent variations. However, when $c > 0.61$ (which represent baroclinicities characteristic of more winter-like conditions) multiple equilibria are present some of which are unstable, or a single unstable equilibrium is present admitting the possiblity of sustained variations. We next discuss the nature of this response assuming a fixed winter-like value of c and then we discuss the case in which we apply a prescribed seasonal variation of c and G implied by (3.10) and (3.11). All time-dependent calculations were made using the fourth order Taylor-series procedure employed by Lorenz (1984), to whom we are grateful for the numerical code.

a. Fixed winter mean conditions

In Fig. 5 we show the time dependent response of the model wave amplitude $A^* = \sqrt{Y^2 + Z^2}$ (which is proportional to the poleward heat transport and conversion between zonal and eddy available potential energy) and zonal mean state, X, when a strongly baroclinic basic state, $c = 1.2$, is prescribed. As shown in Fig. 2, for this value of c the system admits only one spirally-unstable equilibrium. The response is clearly periodic, representing a near-20 day amplitude vacillation. The phase angle of the eastward progressing, vacillating, wave is shown in the last panel.

In Fig. 6a we show the limit cycle trajectory of the solution in the A^* - X plane; the dots are separated by equal time steps, showing by the closeness of the dots where the system tends to reside longer. In order to describe the motion of the vacillating wave in an alternate way to that shown in Fig. 5, we present in Fig. 6b the trajectory of the solution in the Y - Z plane. Noting that the phase angle θ is given by $\theta = \arctan Z/Y$, this figure indicates that the wave progresses eastward, but slows down considerably and is near maximum amplitude when $\theta \approx 90^o$, when the cold trough is near the east coast of the continent and the warm ridge is near the west coast as is often observed. The maximum growth of the wave occurs when there is both near maximum zonal baroclinicity, measured by c, and the wave is in phase with the heating, i.e., when there is a strong cooperation of instability and forcing. The decrease in amplitude occurs more slowly because this is accomplished mainly due to forcing alone as the thermal wave becomes $\sim 180^o$ out of phase with the heating, e.g., as cold air moves out over the warm ocean and the warmer air over the colder continent. The vacillatory progression is schematically illustrated in Fig. 7. While observations suggest that there is indeed some tendency for a near-20 day period vacillation in winter (e.g., McGuirk and Reiter, 1976; Schilling, 1987), such behavior is only intermittent, is clearly not of the regular form pictured

in Figs. 5-7, and is not associated with progressive phase changes due to wave movement (i.e., the waves are nearly stationary). Many factors not considered in this model, however, would act to upset the regularity of the vacillations pictured, e.g., wave-wave interactions, and the blocking effects of mountain ranges that could prevent the eastward progression of warm and cold air masses shown in

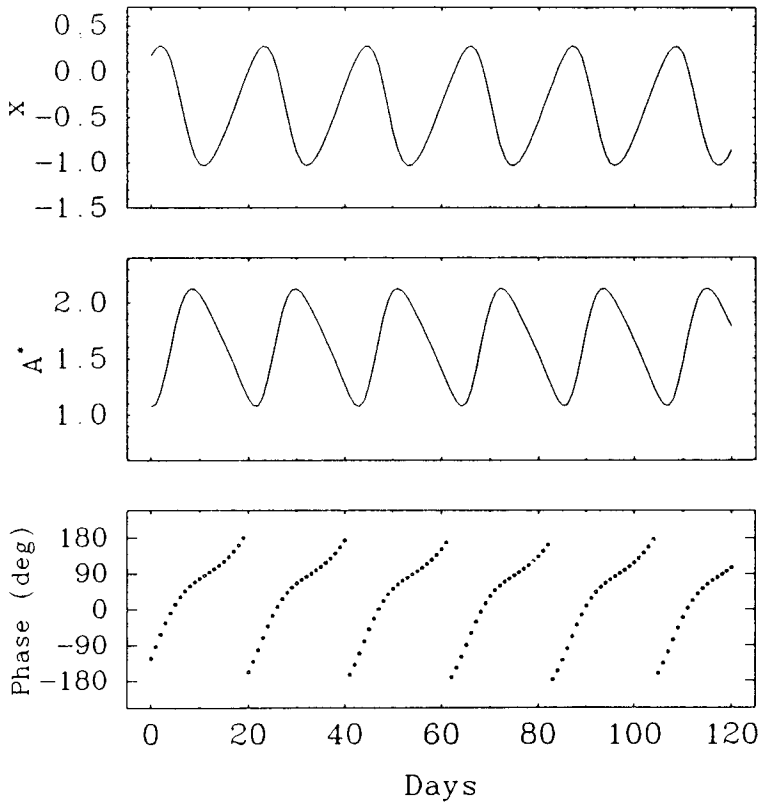

Fig. 5. Time dependent, vacillatory, solution of the system (3.12) - (3.14) for $c = 1.2$ and $G = 0.7$ with all other parameters at their "reference" values. Top panel: free zonal wind structure, or baroclinicity, measured by X; middle panel: wave amplitude, A^*; lower panel: phase angle of the wave, measured by $\theta = \arctan Z/Y$, showing with dots separated by equal time increments that the wave progresses eastward but slows considerably when near $\theta = 90°$.

Fig. 7 particularly with regard to the movement of warm Pacific air masses over North America. Moreover, with sufficient folding of the resonance curve the upper stable equilibrium point will serve as a strong attraction for the system to depart from the limit cycle corresponding to the U_2 unstable equilibrium.

In Fig. 8 we show that with a change in parameters ($c = 1.0$, $G = 1.5$), bringing the system closer to the Hopf bifurcation shown in Fig. 3a, the vacillation can occur with a lower amplitude than the reference case (Fig. 5) and in a more nearly stationary position (roughly 90 degrees out of phase with the heating). In this Figure the dotted lines correspond to the forced "upper" stable equilibrium, while the periodic fluctuations represent a limit cycle (vacillation) about the "lower" unstable equilibrium. We may entertain the possibility that this upper stable, forced, equilibrium

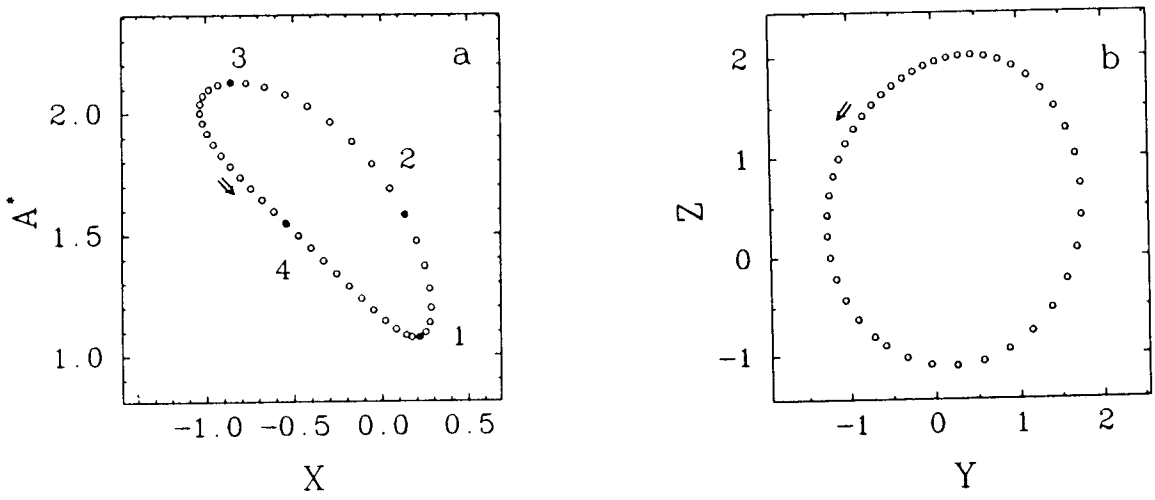

Fig. 6. Trajectory of the time dependent periodic solution shown in Fig. 3 in (a) the $A^* - X$ plane and (b) the $Y - Z$ plane. The dots are separated by equal time intervals, showing by the closeness of the spacing the relative residence time in various regions of the phase planes. The waveforms corresponding to points 1-4 on part (a) are shown in Fig. 7.

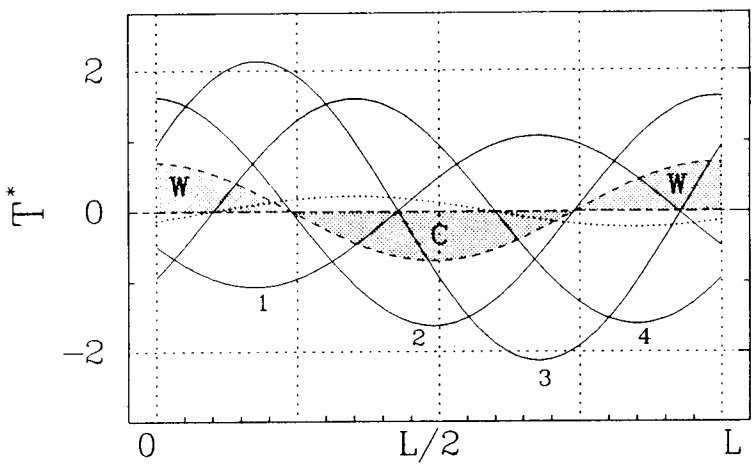

Fig. 7. Vacillatory eastward progression of the thermal wave relative to the fixed (oceanic) warming and (continental) cooling distribution (shaded), denoted by W and C respectively, starting from the low amplitude point 1 on Fig. 6a. T^* is the nondimensional temperature departure defined by $T = \hat{A}T^*$.

corresponds to one of the modes of Sutera (1986) and Hansen (1986), while the other quasi-stationary wave state which the system prefers during the vacillation corresponds to the other mode. While it is likely that, as shown in Fig. 8, the high amplitude mode II is associated with the upper stable branch and the low amplitude mode I is associated with the high residence point on the limit cycle, it is conceivable that the reverse may be true for parameter values that can lead to an amplified limit cycle.

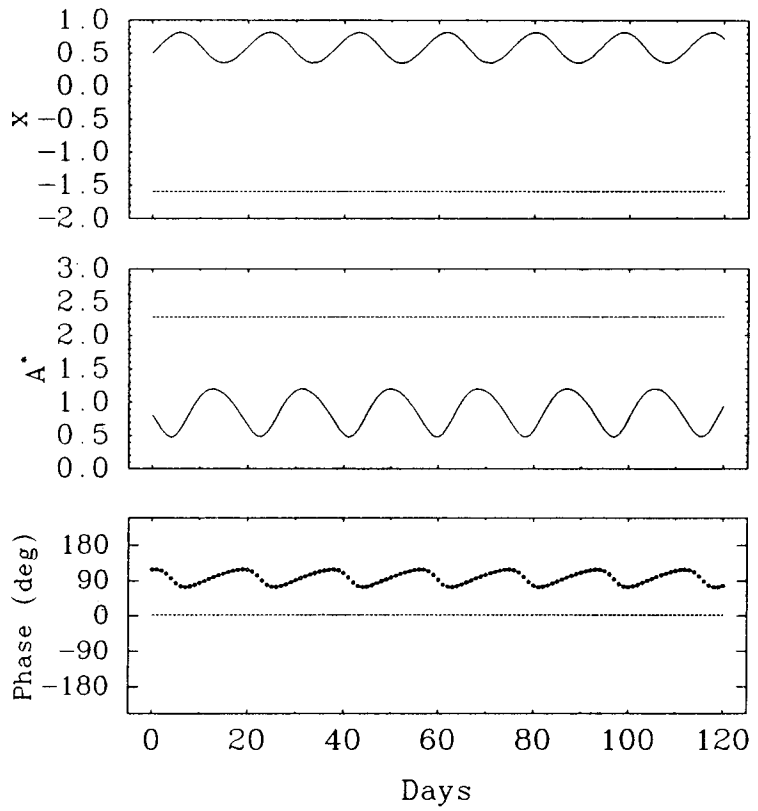

Fig. 8. Same as Fig. 5, but for parameter values $c = 1.0$, and $G = 1.5$. Dotted lines represent the forced "upper" stable equilibrium, while the periodic fluctuations represent a limit cycle around the "lower" unstable equilibrium.

b. Seasonal forcing

As noted in Section 3, we assume that seasonal radiative forcing induces an annual periodic variation only in the basic *linear* part of the north-south surface temperature variation measured by B_{so}, and hence in $c(B_o)$, as represented by (3.10). In addition, a simultaneous annual periodic variation in the east-west (continent-ocean) distribution of surface temperature measured by C_{s2} occurs, leading to the variation in G represented by (3.11).

As an illustration we choose the values $[c_o(B_{oo}), c_1(B_{o1})] = (0.8, 0.4)$ and $[G(\mathcal{G}_o), G(\mathcal{G}_1)] = (0.2, 0.5)$, retaining all other values given in Section 4 for the coefficients of (3.12) - (3.14). We note from Fig. 2 that this annual cycle for c will tend to move the system across the main bifurcations in the fold as the system moves between winter and summer. The results are shown in Fig. 9, the top panel of which gives the general forms of both seasonal forcing functions $c(t)$ and $G(t)$. The response of the wave amplitude, A^*, to this forcing is shown in the second panel, and observations of a related quantity, the conversion of zonal available potential energy to eddy available potential energy $C(A_Z, A_E)$ obtained by Krueger *et al.* (1965), is shown in the next panel. The model seems capable of reproducing qualitatively the emergence of the kind of winter vacillatory variations that are observed. Note also that because of the folded nature of the steady states the response shown is asymmetric with respect to the purely sinusoidal forcing; such an asymmetry is consistent with the discussion

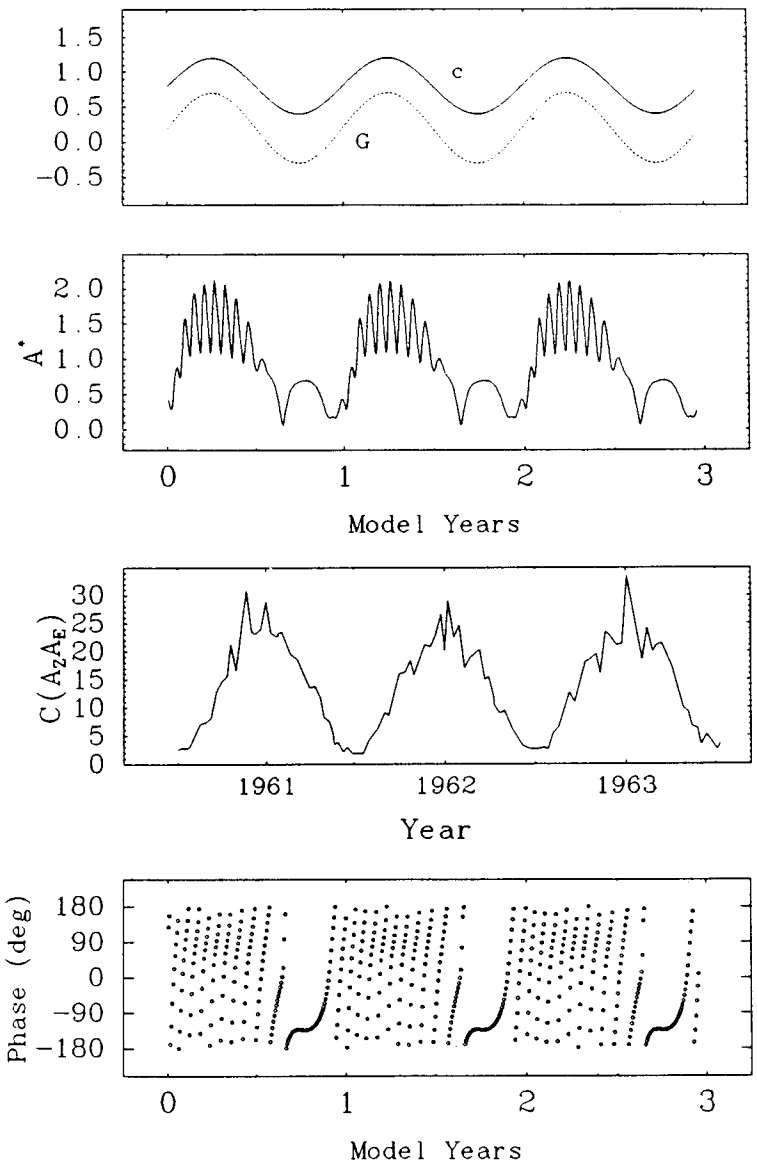

Fig. 9. Time dependent solution of the system (3.12) - (3.14) when forced by the annual cycle of c and G represented by (3.10) and (3.11), respectively, with $(c_o, c_1) = (0.8, 0.4)$, $(G_o, G_1) = (0.2, 0.5)$, and all other parameters at their reference values. Variations of forcing functions c and G in nondimensional units (top panel); variations of the wave amplitude A^*, which is proportional to the meridional heat transport (second panel), to be compared with observations of a related quantity obtained by Krueger *et al.*, 1965 (third panel). The last panel shows the time-variations in the phase angle of the wave, θ, showing summertime stationarity with the warm atmospheric ridge in phase with the warm continent and wintertime eastward progression with prolonged residence when the cold air is over the east coast of the cold continent.

of Kraus and Lorenz (1966) and with observations of the seasonal cycle of quasi-stationary thermal waves (e.g., Oort and Rasmusson, 1971, pp. 114-115). From the phase evolution shown in the last panel we see that in summer the low amplitude wave is nearly in phase with the continent-ocean heating distribution, and in winter the vacillating wave moves eastward but slows down considerably when the phase is such that the cold air is over the east coast of the continent perhaps, as discussed above, constituting one of the two preferred modes. As also noted above, this vacillatory mode is vulnerable to attraction by the forced stable steady state that may constitute the other mode. When wave-wave interactions are included, as suggested by Benzi *et al.* (1987) and Hansen (1988) for example, a more realistic time evolution might be expected including the mode to mode transitions

and the relative phase stationarity of the two modes.

6. Conclusions

In this study we have formulated a three component, non-linear dynamical system aimed at modelling aspects of the thermally forced dissipative, baroclinic, planetary middle latitude flow. The model can be viewed as a slightly more general form of the Lorenz (1984) model. In this connection it is well known that such a 3-component system already potentially contains great complexity in the form of periodic and aperiodic behavior (Lorenz, 1984) and is worthy of detailed further study before adding too many additional components.

Specifically we have ilustrated a long-wave dynamical scenario involving thermal forcing and seasonal cycle effects in the absence of any orographic forcing, the main properties of which arise from the existence of multiple equilibria associated with a "folded resonance" as a function of the basic forced baroclinic state. This folded kind of equilibrium structure is suggestive of the type needed to account for recent observations (Sutera, 1986; Hansen, 1986) showing that the planetary waves are baroclinic and have a *bimodal* amplitude structure corresponding to a unimodal basic zonal wind. To the extent that this model is valid, one mode might be viewed as a baroclinically-amplified, thermally-forced quasi-vacillatory wave having a long residence time at the observed phase relative to the continents. On the other hand the other mode might be identifiable with the non-amplified diabatically-maintained wave constituting the upper stable equilibrium in our model. As a consequence of this equilibrium structure, as the external forcing maintaining the basic temperature gradient is varied the system can undergo an interesting sequence of bifurcations in a realistic baroclinic domain showing the wintertime emergence of an asymmetric quasi-vacillatory behavior qualitatively similar to that reported by Krueger *et al.* (1965) and studied numerically by Kraus and Lorenz (1966).

While these results are of interest, suggesting the potential relevance of the physical mechanisms included, other lines of evidence concerning the wave-wave energetics (Hansen and Sutera, 1984) and other theoretical considerations (e.g., Held, 1983) tend to raise questions concerning quasi-resonant mechanism as a full explanation of the observations. However, some new ideas put forth by Benzi *et al.* (1986a,b, 1987), and Speranza (1986) involving the potentially critical role of baroclinic wave-wave interactions encourage the hope that a more acceptable minimum model to account for the observed bimodality and transient properties, harmonizing all of the previous results, can be constructed.

Acknowledgements

This research was supported by the Global Scale Atmospheric Processes Research Program of the National Aeronautics and Space Administration under contracts NAS8-36356 at Yale University and NAS8-37130 at the Universities Space Research Association.

APPENDIX A

Determination of the fixed points and their stability

A1. Steady states

In the study of nonlinear dynamical systems analytical solutions for the time dependent behavior, as well as determination of steady states and their linearized stability (eigenvalues) are impractical. Such is the case for the thermally-forced baroclinic wave model described in this paper. In order

to gain an idea of how steady states and stability vary as a funtion of changing a parameter of the model one must resort to numerical computation. The model in nondimensional form, given in the text by equations (3.12) - (3.14), was reduced to a single equation (4.6) for steady state values of X of the form

$$a(F-\hat{X})\{[e\hat{X}+K_2(B_0)]^2+[K_1\hat{X}+K_3(B_o)]^2\}=G^2.$$

Substituting into (4.6) for K_2 and K_3 in terms of c (i.e., $K_2=[c(B_o)-1]$ and $K_3=[(b^*-\epsilon)c(B_o)-d]$) and expanding gives the following cubic in $\hat{X}$:

$$\underbrace{[-aK_1^2-ae^2]}_{\mathcal{A}}\hat{X}^3+\underbrace{[aFK_1^2-2a(c(b^*-\epsilon)-d)K_1+ae^2F-2a(c-1)e]}_{\mathcal{B}}\hat{X}^2$$

$$+\underbrace{[2a(c(b^*-\epsilon)-d)FK_1+2a(c-1)eF-a(c(b^*-\epsilon)-d)^2-a(c-1)^2]}_{\mathcal{C}}\hat{X}$$

$$+\underbrace{[a(c(b^*-\epsilon)-d)^2F+a(c-1)^2F-G^2]}_{\mathcal{D}}=0 \qquad (A.1)$$

The solutions to this equation for $\hat{X}$ along with substitution back into equations (4.4) and (4.5) to obtain the corresponding values for $\hat{Y}$ and $\hat{Z}$ give us the steady states for any given set of model coefficients. Since only real steady states have physical meaning we need not concern ourselves with complex solutions and so to solve equation (A.1) we will first check to see whether it has only one real root or three. Define Q and R in terms of $\mathcal{A}$, $\mathcal{B}$, $\mathcal{C}$ and $\mathcal{D}$ as follows (Press *et al.*, 1986):

$$Q\equiv\frac{(\mathcal{B}/\mathcal{A})^2-3(\mathcal{C}/\mathcal{A})}{9} \qquad \text{and}$$

$$R\equiv\frac{2(\mathcal{B}/\mathcal{A})^3-9(\mathcal{B}/\mathcal{A})(\mathcal{C}/\mathcal{A})+27(\mathcal{D}/\mathcal{A})}{54}$$

When $Q^3-R^2\geq 0$ all three roots are real and may be found by calculating $\vartheta=\arccos(R/\sqrt{Q^3})$ and substituting along with Q, $\mathcal{A}$ and $\mathcal{B}$ into

$$\hat{X}_1=-2\sqrt{Q}\cos(\frac{\vartheta}{3})-(\mathcal{B}/\mathcal{A})/3$$

$$\hat{X}_2=-2\sqrt{Q}\cos(\frac{\vartheta+2\pi}{3})-(\mathcal{B}/\mathcal{A})/3$$

$$\hat{X}_3=-2\sqrt{Q}\cos(\frac{\vartheta+4\pi}{3})-(\mathcal{B}/\mathcal{A})/3.$$

However, if $Q^3-R^2<0$ then only one root is real and is given by

$$\hat{X}=-\text{sgn}\left[(\sqrt{R^2-Q^3}+|R|)^{(1/3)}+\frac{Q}{(\sqrt{R^2-Q^3}+|R|)^{(1/3)}}\right]-(\mathcal{B}/\mathcal{A})/3$$

Due to the fact that numerical round-off may be significant in the calculation of $\hat{X}$ we will take these solutions as an initial guess, and then use a standard Newton-Raphson method to converge to a more accurate estimate of the steady states. When we substitute our calculations for $\hat{X}$, $\hat{Y}$, and $\hat{Z}$ back into the original equations for $\dot{X}$, $\dot{Y}$, and $\dot{Z}$ they are each satisfied to at least $O(10^{-17})$.

A2. Stability

The stability of these steady states can then be determined by calculating eigenvalues. This is done by linearizing the system in the vicinity of the steady state and then finding solutions of the form $\vec{r}\, e^{\lambda t}$ where λ is the eigenvalue and $\vec{r}$ the corresponding eigenvector. In matrix form the problem we must solve is simply $(\mathbf{J} - \lambda \mathbf{I})\vec{r} = 0$, $\mathbf{J}$ being the Jacobian matrix and $\mathbf{I}$ the identity matrix. This can only be true for $\vec{r} \neq 0$ (i.e., non-trivial solutions) if det ($\mathbf{J}$ - λ $\mathbf{I}$) = 0, which for equations (3.12) - (3.14) means

$$\begin{vmatrix} -a-\lambda & -2\hat{Y} & -2\hat{Z} \\ e\hat{Y} - K_1\hat{Z} & e\hat{X} + (c-1) - \lambda & -K_1\hat{X} - [(b^* - \epsilon)c - d] \\ e\hat{Z} + K_1\hat{Y} & K_1\hat{X} + [(b^* - \epsilon)c - d] & (c-1) + e\hat{X} - \lambda \end{vmatrix} = 0$$

The numerical solution of this determinant is then found using EISPACK subroutines (Garbow *et al.*, 1977). As a check we then expand the determinant and use the fact that $\hat{Y}^2 + \hat{Z}^2 = a(F - \hat{X})$ to obtain a cubic equation in λ of the form

$$\lambda^3 + \{a - 2[e\hat{X} + (c-1)]\}\lambda^2 +$$

$$\{(e\hat{X} + (c-1))^2 + (K_1\hat{X} + ((b^* - \epsilon)c - d))^2 +$$

$$2a[e(F - \hat{X}) - (e\hat{X} + (c-1))]\}\lambda +$$

$$\{a[(e\hat{X} + (c-1))^2 + (K_1\hat{X} + (b^* - \epsilon)c - d)^2] -$$

$$2a(F - \hat{X})[e(e\hat{X} + (c-1)) + K_1(K_1\hat{X} + (b^* - \epsilon)c - d)]\} = 0$$

into which we can then substitute the eigenvalues found using EISPACK.

REFERENCES

Benzi, R., P. Malguzzi, A. Speranza and A. Sutera, 1986. The statistical properties of general atmospheric circulation: observational evidence and a minimal theory of bimodality. *Quart. J. R. Met. Soc.*, **112**, 661-674.

Benzi, R. A., A. Speranza and A. Sutera, 1986. A minimal baroclinic model for the statistical properties of low-frequency variability. *J. Atmos. Sci.*, **43**, 2962-2967.

Benzi, R., S. Iarlori, P. Malguzzi, A. Speranza and A. Sutera, 1987. A minimal theory of transitions between large and small wave amplitude modes and atmospheric bimodality. (Manuscript submitted for publication).

Derome, J. and A. Wiin-Nielsen, 1971. The response of a middle-latitude model atmosphere to forcing by topography and stationary heat sources. *Mon. Weath. Rev.* **99**, 564-576.

Döös, B. R., 1962. The influence of exchange of sensible heat with the Earth's surface on the planetary flow. *Tellus*, **14**, 133-147.

Egger, J., 1981. Stochastically driven large-scale circulation with multiple equilibria. *J. Atmos. Sci*, **38**, 2606-2618.

Garbow, B., J. Boyle, J. Dongarra and C. Molar, 1977. Matrix eigensystem routines - EISPACK guide extension, Lecture Notes in Computer Science, Springer-Verlag, New York.

Hansen, A. R., 1986. Observational characteristics of atmospheric planetary waves with bimodal amplitude distributions. *Adv. in Geophys.*, **29**, 101-133.

Hansen, A. R., 1988. Further observational characteristics of bimodal planetary waves: mean structure and transitions. *Mon. Weath. Rev.*, **116**, 386-400.

Hansen, A. R., and A. Sutera, 1986. On the probability density distribution of planetary-scale atmospheric wave amplitude. *J. Atmos. Sci.*, **43**, 3250-3265.

Held, I. M., 1983. Stationary and quasi-stationary eddies in the extratropical troposphere: theory. *Large Scale Dynamical Processes in the Atmosphere* (B. Hoskins and R. Pearce, eds.) Acad. Press, 127-168.

Hendon, H. H., 1986. Time-mean flow and variability in a nonlinear model of the atmosphere with orographic forcing. *J. Atmos. Sci.*, **43**, 433-488.

Kraus, E. B. and E. N. Lorenz, 1966. Numerical experiments with large-scale seasonal forcing. *J. Atmos. Sci.*, **23**, 3-12.

Krueger, A. F., J. S. Winston and D. H. Haines, 1965. Computations of atmospheric energy and its transformation for the northern hemisphere for a recent five-year period. *Mon. Weath. Rev.*, **93**. 227-238.

Lorenz, E. N., 1984. Irregularity: A fundamental property of the atmosphere. *Tellus*, **36A**, 98-110.

Lorenz, E. N., 1987. Deterministic and stochastic aspects of atmospheric dynamics. *Irreversible Phenomena and Dynamical Systems Analysis in Geosciences* (C. Nicolis and G. Nicolis, eds.), D. Reidel Publ. Co., 159-179.

Malguzzi, P. and A. Speranza, 1981. Local multiple equilibria and regional atmospheric blocking. *J. Atmos. Sci.*, **38**, 1939-1948.

McGuirk, J. P. and E. R. Reiter, 1976. A vacillation in atmospheric energy parameters, *J. Atmos. Sci.*, **33**, 2079-2093.

McWilliams, J. C. and P. R. Gent, 1980. Intermediate models of planetary circulations in the atmosphere and ocean. *J. Atmos. Sci.*, **37**, 1657-1678.

Neelin, J. D., I. M. Held and K. H. Cook, 1987. Evaporation-wind feedback and low-frequency variability in the tropical atmosphere. *J. Atmos. Sci.*, **44**, 2341-2348.

Oort, A. H. and E. M. Rasmusson, 1971. *Atmospheric Circulation Statistics*, NOAA Prof. Pap. 5, 323 pp.

Press, W. H., B. P. Flannery, S. A. Teukolsky and W. T. Vetterling, 1986. *Numerical Recipies the Art of Scientific Computing*, Cambridge Unviresity Press, New York, p. 146.

Ramanathan, V., 1987. The role of earth radiation budget studies in climate and general circulation research. *J. Geophys. Res.*, **92, D4,** 4075-4095.

Rambaldi, S. and K. C. Mo, 1984. Forced stationary solution in a barotropic channel: multiple equilibria and theory of non-linear resonance. *J. Atmos. Sci.*, **41**, 3135-3146.

Saltzman, B., 1965. On the theory of the winter-average perturbations in the troposphere and stratosphere. *Mon. Weath. Rev.*, **93**, 195-211.

Saltzman, B. and A. D. Vernekar, 1968. A parameterization of the large-scale eddy flux of relative angular momentum. *Mon. Weath. Rev.*, **96**, 854-857.

Schilling, H-D., 1987. Observed baroclinic energy conversions in wavenumber domain for three winters: A time series analysis, *Mon. Weath. Rev.*, **115**, 520-538.

Smagorinsky, J., 1953. The dynamical influence of large-scale heat sources and sinks on the quasi-stationary mean motions of the atmosphere. *Quart. J. R. Met. Soc.*, **79**, 342-366.

Speranza, A., 1986. Deterministic and statistical properties of Northern Hemisphere, middle latitude circulation: minimal theoretical models. *Adv. in Geophysics*, **29**, 199-225.

Sutera, A., 1986. Probability density distribution of large-scale atmospheric flow. *Adv. in Geophysics*, **29**, 227-249.

Trevisan, A. and A. Buzzi, 1980. Stationary response of barotropic weakly nonlinear Rossby waves to quasi-resonant orographic forcing. *J. Atmos. Sci.*, **37**, 947-957.

Yoden, S., 1987. Bifurcation properties of a stratospheric vacillation model. *J. Atmos. Sci.*, **44**, 1723-1733.